Preferred citation: M.B. Lyne. On the interaction of liquids with paper under dynamic conditions. In **Products of Papermaking**, *Trans. of the Xth Fund. Res. Symp. Oxford, 1993*, (C.F. Baker, ed.), pp 885–911, FRC, Manchester, 2018. DOI: 10.15376/frc.1993.2.885.

ON THE INTERACTION OF LIQUIDS WITH PAPER UNDER DYNAMIC CONDITIONS

M. Bruce Lyne
Royal Institute of Technology
Drottning Kristinas väg 53
S-100 44 Stockholm, Sweden

ABSTRACT

Some recent advances in understanding the dynamic interactions of liquids with solid surfaces are reviewed. Specifically, acid-base theory is applied to wetting and adhesion, the meaning of precursor films for spreading is examined, the role of pore morphology in capillary penetration is explored theoretically and experimentally, adsorption and spreading of surfactant solutions is compared to that of aqueous alcohol solutions, three dimensional pressure penetration models are described along with new methods for characterizing penetration and pore size distribution, and means of reducing fiber swelling and the hygroreactivity of paper and board is discussed.

INTRODUCTION

Liquids interact with paper under a variety of conditions during printing and converting operations and during ultimate end-use. Satisfactory performance in these situations can entail a specific resistance to pressure penetration, rapid wetting and capillary penetration, limited spreading and an absence of wicking, and filtration or chromatographic separation of the components of the liquid. Diffusion of polar liquids such as water into fiber walls causes swelling and network expansion which is an issue of considerable importance for color registration in offset lithography and in water-based flexography and gravure printing, as well as for penetration of highly densified papers. A key factor in printing and converting is whether significant penetration of the fiber wall occurs on a time scale which is shorter than the duration of the paper handling process.

The macro structure of the surface and bulk pore system in paper, together with micro scale roughness and porosity, and local surface energetics are the chief determinants of these interactions with liquids. Understanding these relationships and their implications for the performance of paper and board products should aid in troubleshooting problems in the field, facilitate design of products with an optimum balance of properties, and lead the way in the development of new materials needed to achieve superior performance.

For purposes of discussion, liquid-paper interactions have been divided into the following phenomena:

-dynamic wetting, spreading, and capillary penetration
-pressure penetration
-diffusion into the fiber wall and swelling

DYNAMIC WETTING, SPREADING, AND CAPILLARY PENETRATION

Wetting can be viewed as an interfacial adhesion phenomenon between a liquid and a solid surface. There are two basic types of intermolecular interactions that contribute to wetting and adhesion: dispersive and acid-base. Dispersive forces are weak attractions between fluctuating dipoles that operate at relatively long range (in excess of one hundred Angstroms). These forces, which are referred to as London-van der Waals or Lifshitz-van der Waals forces, are apolar interactions where the electromagnetic field created by random fluctuations in the dipole moment of a molecule induce a corresponding fluctuation in a neighboring molecule and attraction across the liquid-solid phase boundary.

In contrast, acid-base interactions involve fixed overlap of electron densities, or electron donor-acceptor exchange between two molecules on

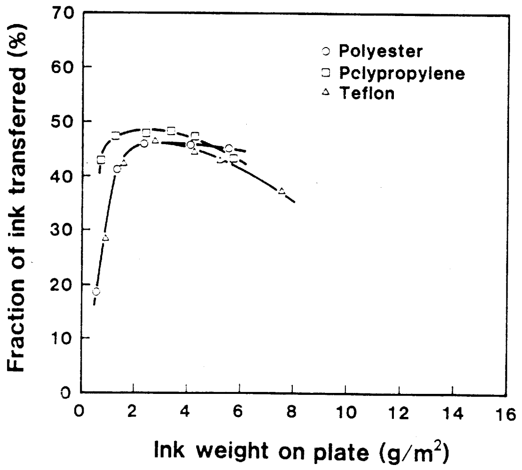

FIG: 1 Fraction of oil-based ink transferred from printing plate to polymer sheets in a GFL rotary printing press. DeGrace and Mangin (34).

Hydrophilicity and Acid-Base Interactions

Substrate	γ_S^d (mN/m)	Contact Angle with Water (deg.)	W_A (mJ/m²)	W_A^d (mJ/m²)	W_A^{ab} (mJ/m²)
Glass	76.0	0	145.6	81.4	64.2
Cellophane (50% RH)	48.6	28	137.1	65.1	72.0
(95% RH)	41.6	5	145.3	60.2	85.1
PMMA	36.1	74	92.9	56.1	36.8
Polyethylene	33.1	105	54.0	53.7	0.7
Polypropylene	28.4	108	50.3	49.8	0.5
Teflon	19.0	116	40.9	40.7	0.2

For Water: $\gamma_{LV} = \gamma_L^d(21.8) + \gamma_L^{ab}(51.0) = 72.8$ mN/m

Table 1 Hydrophilicity and Acid Base interactions between water and cellulose opposite sides of the phase boundary. Acid-base interactions are much stronger than dispersive forces, but they act over shorter ranges (as little as 5 Angstroms), and thus require intimate conformation of the liquid to the solid surface.

Wetting is generally studied under equilibrium conditions and reported as a static interfacial contact angle. However, liquids that are forced into contact with solids under pressure will wet and adhere even though non-wetting occurs under equilibrium conditions. This is important in industrial processes such as printing where critical liquid transfer processes occur in nips under pressure. As shown in Figure 1, the transfer curves for mineral oil based ink to polytetrafluoroethylene (Teflon) and transfer curves to polypropylene and polyester are the same although the critical surface free energies are 18, 35, and 42 mN/m, respectively. In fact, mineral oil forms a high contact angle with Teflon under equilibrium conditions and the ink beads up on the Teflon after the printing nip. In general, when pressure is applied to force a liquid into intimate contact with a solid surface dispersive interactions are enhanced and wetting may occur when not energetically favorable under equilibrium conditions.

Aspler et al. (1) demonstrated that water-based inks behave differently than oil-based inks regarding the effect of the surface chemistry of paper on ink transfer. Alkaline water-based flexographic inks transferred better as the acidity of the paper was increased and as the paper became more hydrophilic (at the same roughness). Thus, acid-base interactions and wettability seem to play a role in the transfer of water-based inks.

The work of adhesion (W_A) between a liquid and a solid surface can be written as:

$$W_A = \gamma_{LV} + \gamma_{SV} - \gamma_{SL} \tag{1}$$

in which γ is the symbol for surface tension and the subscripts L, V, and S denote liquid, vapor, and solid, respectively. Substituting the Young-Dupré contact angle equation and assuming negligible equilibrium spreading pressure, the work of adhesion can also be expressed as:

$$W_A = \gamma_{LV}(1 + \cos\theta). \tag{2}$$

Recently, it has become common to partition the work of adhesion into dispersive and acid-base interactions as proposed by van Oss, et al. (2):

$$W_A = 2[(\gamma_S^d \gamma_L^d)^{1/2} + (\gamma_S^{\oplus} \gamma_L^{\ominus})^{1/2} + (\gamma_S^{\ominus} \gamma_L^{\oplus})^{1/2}] \quad (3)$$

in which the superscripts d, $\oplus$, and $\ominus$ denote contributions to surface free energy from dispersion forces, and acidity (electron acceptor) and basicity (electron donor), respectively. Thus, knowing the dispersive, acid, and base components of the surface free energy of the solid and liquid it is possible to calculate the dispersive and acid-base components of their adhesive interaction. If probe liquids having known dispersive, acid and base components are applied to a solid and the contact angles determined, it is possible to calculate the dispersive, acid, and base characteristics of the solid.

Lyne and Huang (3) were able to extend this technique to paper using the Bristow wheel to calculate dynamic advancing contact angles between pore walls and the probe liquids. They observed that the purely dispersive probe had to have a contact angle close to 90 degrees in order to arrive at correct values for the dispersive component of the paper surface. Probe liquids with lower contact angles gave anomalously high values for the dispersive component for paper indicating the importance of capillary pressure in forcing the liquid into more intimate contact with the surface of the pore walls. This effect of capillary pressure on dispersive interactions was further studied by Huang and Lyne (4) in experiments where the pore size in the paper was varied. The calculated dispersive component for the surface of the pore walls was found to be inversely related to the average pore diameter (i.e., linearly related to the capillary pressure).

The effects of dispersive and acid-base interaction on wetting can be illustrated by comparing the way in which water and cyclohexane wet polyethylene and glass. Since polyethylene has no acid or base component interactions with water and cyclohexane are purely dispersive. Since the dispersive component for cyclohexane is greater than that for water (25.5 and 21.8 mN/m, respectively) cyclohexane wets polyethylene and water does not. Conversely, glass like water has pronounced acid-base characteristics in addition to a dispersive component. It follows that the overall work of adhesion between water and glass is larger than the work of adhesion between a purely dispersive liquid such as cyclohexane and glass. Thus, water wets glass more aggressively. This can be further appreciated in Table I where the static contact angle between water and glass, and between water and various polymers can be compared with the dispersive and acid-base components of the work of adhesion between water and these surfaces. As a general rule of thumb, the total work of adhesion between a solid and a liquid must exceed 100 mN/m for wetting to occur under equilibrium conditions.

On a molecular level it seems improbable that a liquid would end abruptly at the three phase line, as predicted by the Young-Dupré equation. In fact, it has been known since the work of Hardy (5) in 1919 that a thin film of liquid precedes the complete spreading of a drop or bulk liquid on a solid surface. Hardy noted that two drops of acetic acid would preferentially move towards one another if separated by less than one or two centimeters. Similarly, Marmur and Lelah (6) demonstrated that the rate of spreading of aqueous solutions on glass slides was much higher for smaller pieces of glass, and that the effect asymptotically diminished as the glass square increased above 8 centimeters. They observed the rate of spreading of the precursor film to be in the order of 10 cm/s and reasoned that limiting the size of the glass square causes a gradient in the thickness of the precursor film and that the resulting gradient in surface tension in the film drives the spreading rate upwards. While ellipsometry has revealed the presence of precursor films it is still not entirely clear, as pointed out by Léger et al. (7), what the degree of order is in these films or whether they behave as normal liquids at all.

Spreading is deemed to be energetically favorable when the net surface energy is decreased by coverage of the solid with the liquid. This is expressed in Young's spreading equation as:

$$S = W_A - W_C = \gamma_{SV} - \gamma_{LV} - \gamma_{SL} \qquad (4)$$

where S is the spreading coefficient and W_C is the work of cohesion which is equal to twice the value of γ_{LV}.

However, de Gennes (8) theorized that the spreading kinetics of a liquid on a solid should be independent of the spreading coefficient S due to the dissipation of the excess free energy in the precursor film. Intuitively, one would expect the energetics driving the spreading of a low surface free energy liquid on a solid surface would be diminished by the adsorption of a precursor film or adsorption of the liquid's vapor on the solid surface. Lelah and Marmur (9) have shown that water behaves differently in that spreading is enhanced by increasing the ambient relative humidity. This is

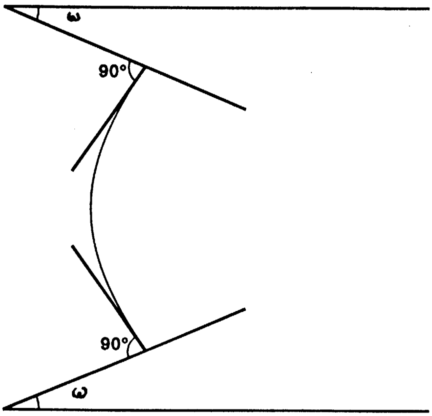

FIG. 2 Capillary penetration into a conical pore having a convergence angle ω where contact angle with capillary walls equals 90 degrees. Kent and Lyne (14).

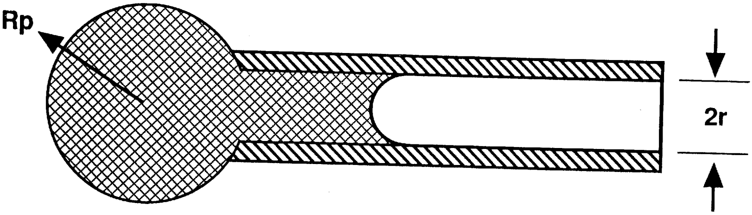

FIG. 3 Penetration of liquid from a finite reservoir of radius Rp into a capillary of radius r, where the total capillary pressure equals $\frac{2\gamma}{R_P}+\frac{2\gamma\cos\theta}{r}$. Marmur (17).

also known for the spreading and penetration of water on cellulose and paper as demonstrated by Lyne and Aspler (10). The explanation of this behavior may lie in Table I where it can be seen that the acid-base interaction between water and cellulose predominates in wetting, and that it increases with relative humidity. Similarly, the receding contact angle for water on pre-wetted cellulose surfaces has been reported by Borgin (11) to always be zero. In other words, more acid-base sites on the cellulose surface become active as relative humidity is increased.

As shown by Oliver and Mason (12), spreading is enhanced by rough surfaces for liquids that have contact angles less than ninety degrees, and spreading is inhibited by rough surfaces for contact angles greater than ninety degrees. Further, spreading is enhanced along grooves and inhibited across them. For example, a drop will elongate in the direction of grooves in the surface of a gramophone record. Wetting liquids also tend to wick along fibers in the surface of paper. This behavior can be inhibited by making the paper surface sufficiently hydrophobic that the contact angle is slightly greater than 90 degrees and then increasing micro roughness by pigmenting the surface of the paper.

Cazabat and Cohen Stuart (13) have described the spreading of drops on rough surfaces in four steps: the drop moves as a whole, then a "foot" of liquid finds navigable channels into the roughness and precedes a "cap", then the drops move as whole again, and finally, spreading slows as the drop thickness becomes much smaller than the scale of the roughness. Expansion of the drop radius varied with time, t, as $t^{1/8}$ in the first phase, $t^{1/4}$ in the middle phase, and then slowed to $t^{1/6}$ at the final phase. The authors were also able to model the effects of the maximum roughness on the rate of advance in the middle phase. While such spreading phenomena are indeed complex, they appear to be yielding to the analysis proposed by de Gennes (8).

Contact angle with pore walls is not only a function of the dispersive and acid-base chemistry of the liquid and solid surfaces, but also of pore wall geometry. As shown in Figure 2 from Kent and Lyne (14) the angle of convergence of the pore wall should be subtracted from the contact angle of the liquid with a flat surface of the same material when calculating capillary suction pressures. Thus, a liquid which exhibits a contact angle greater

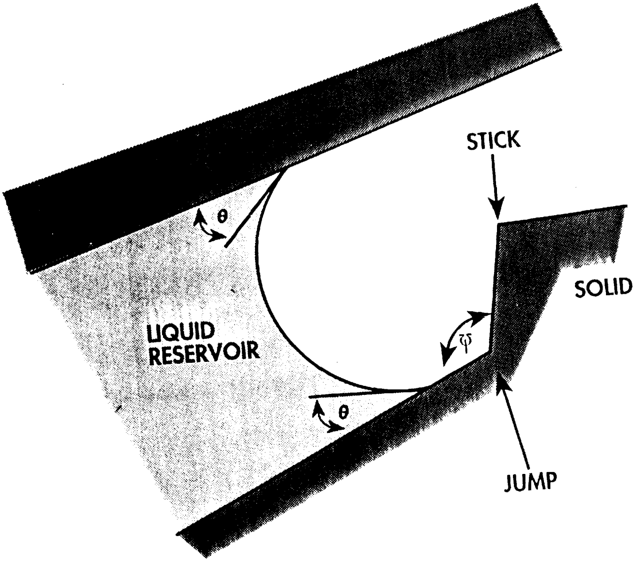

FIG. 4 Acceleration of liquid into a converging pore, jump in velocity at a dislocation of less than 180 degrees, and stick at sharp dislocations greater than 180 degrees. Kent and Lyne (14).

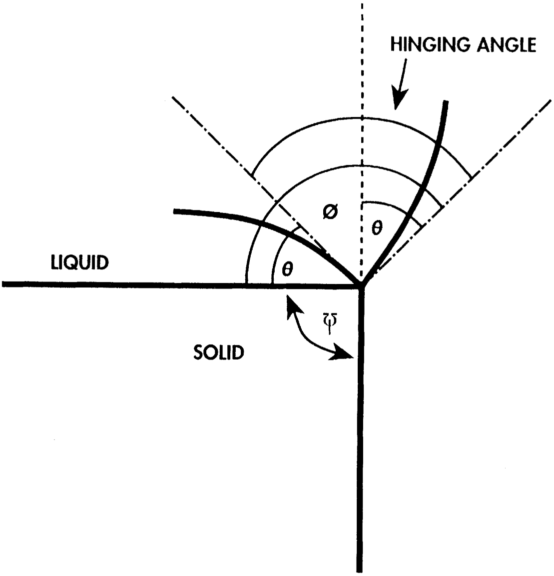

FIG. 5 Hinging behavior of a liquid at a sharp discontinuity. Kent and Lyne (35).

Mineral	Fine Kaolin	Std. Kaolin	Mica	Precipitated Silicoalumnate	Ground Calcium Carbonate
Shape	Platey	Platey	Platey	Amorphous	Blocky
Aspect Ratio	10	15	25	1	1
Mean E.S.D. µm	1	2	10	1	2
Bristow ABS. Rate mL/m²/√s	6	16	190	170	30
Hg. Intrusion Pore Diameter µm	0.4	0.6	0.6	0.6	2.5

Table 2 Structure and rate of oil absorption for five pigments coated on millipore filters with a starch binder

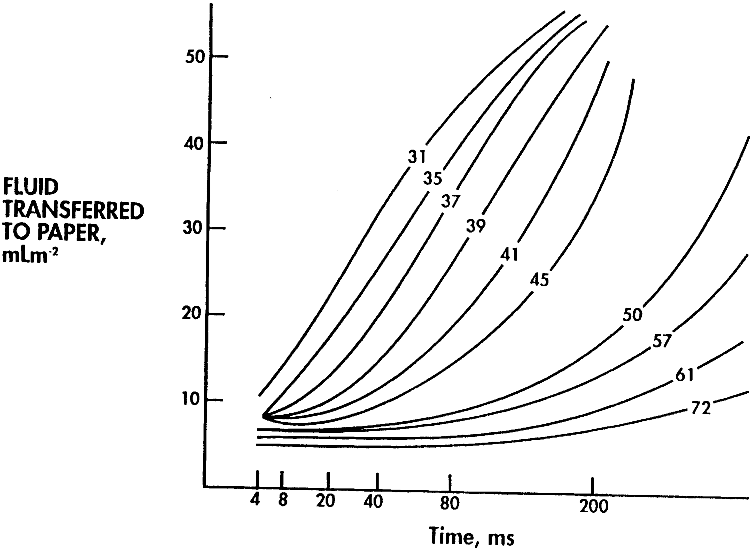

FIG. 6 Absorption curves for water, and for water with increasing amounts of isopropyl alcohol. Surface tension shown on each curve in mN/m. Aspler, Davis, and Lyne (36).

than 90 degrees with a flat film of cellulose can still penetrate the surface pores of a cellulose fiber network since these pores are generally convergent and can be modelled as truncated cones (Corte and Kallmes [15]). This explains why water, which exhibits an initial contact angle with sized paper that exceeds 90 degrees (Okayawa et al. [16]), penetrates the surface pores in a Bristow test (see Lyne and Aspler [10]) without any measurable delay. Marmur (17) has also pointed out that in realistic sorption situations the fluid reservoir is often limited and has a curvature of its own. As shown in Figure 3, if a discontinuous film of liquid is applied to paper as in a printing situation the curvature of the liquid reservoir above the pore also exerts a pressure that speeds capillary penetration.

With irregularly shaped pore walls, capillary penetration can be observed to accelerate in converging portions of the pore and decelerate in diverging portions. As shown in Figure 4 this is a reflection of the change in capillary pressure as calculated by inserting the local contact angle between the liquid front and the pore walls into the Kelvin equation. A further complexity in capillary penetration can also be observed at sharp dislocations in the pore wall as might be encountered at the edge of a mineral filler particle. The liquid can be observed to stick at this point and hinge around the dislocation. As pictured in Figure 5 this behavior is governed by the Gibbs inequality (18) and represents a suspension of the Young-Dupré contact angle equation. If and when the liquid reaches the second surface, capillary suction and penetration resumes.

In mineral coatings and filled papers the frequency of these dislocations and divergent pore geometries are more important in determining penetration rate than pore size. This is illustrated in Table II for five pigments coated on millipore filters with a starch binder. Note that the penetration rate for oil in the Bristow test is much slower for the very porous ground calcium carbonate than for the large plate mica. Presumably, this is due to the frequency of diverging pore sections in the gravel-like carbonate and the frequency of convergent pores in the mica. Since the samples were uncalendered, disorder in plate alignment results in a wide end and a narrow end to the pores between the plates Oil penetrates rapidly from the wide to narrow ends of these pores.

As legislation forces the removal of volatile organic liquids from inks, fountain solution, and varnishes, new problems arise from unwanted sorption and spreading behavior. For example, as shown in Figure 6 isopropanol was very effective in speeding wetting and absorption of fountain solution into paper. While surfactants can also reduce the surface tension of fountain solution they can take more than a second to migrate to the surface of a newly split film of fountain solution as would be found on the outgoing side of a printing nip. As shown in Figure 7 the equilibrium surface tension of a surfactant solution and a solution of isopropanol in water can be the same, but the dynamic surface tension of the surfactant solution can remain the same as that of water for such a long time that little effect is seen on the speed of penetration in the Bristow test. Papers that exhibit a slow rate of absorption for fountain solution may be problematic for the transfer of oil-based ink in subsequent printing nips.

Further, when alcohol evaporates from a water-based ink or fountain solution the remaining liquid increases in surface tension. Conversely, when water evaporates from an ink or fountain solution containing a surfactant the surface tension of the remaining liquid is decreased as the surfactant becomes more concentrated. If an uneven layer of ink or fountain solution is transferred to a paper or board the thin areas will become higher in surface tension for the case of evaporating alcohol, but the thin areas will decrease in surface tension with the evaporation of water from a surfactant solution. Thus, the thick areas move towards thin areas for the alcohol solution, while the thin areas migrate to the thick areas for the surfactant solution. The net result can be a worsening of the nonuniformity in thickness of a surfactant solution. This is particularly grievous for water-based inks since perceived mottle will increase with migration from the thin areas having low surface tension.

Flow caused by gradients in surface tension, as occurs along the sides of a whiskey glass with evaporation of the alcohol, is a manifestation of the Marangoni effect. This is distinct from diffusion caused by concentration gradients and is simply an example of migration that leads to minimization of the total surface free energy of the system.

Borhan et al. (19) examined the drying of water-based inks containing a glycol cosolvent commonly used as a humectant in ink jet inks to prevent ink drying at the ink jet orifice. By increasing stepwise the amount of glycol

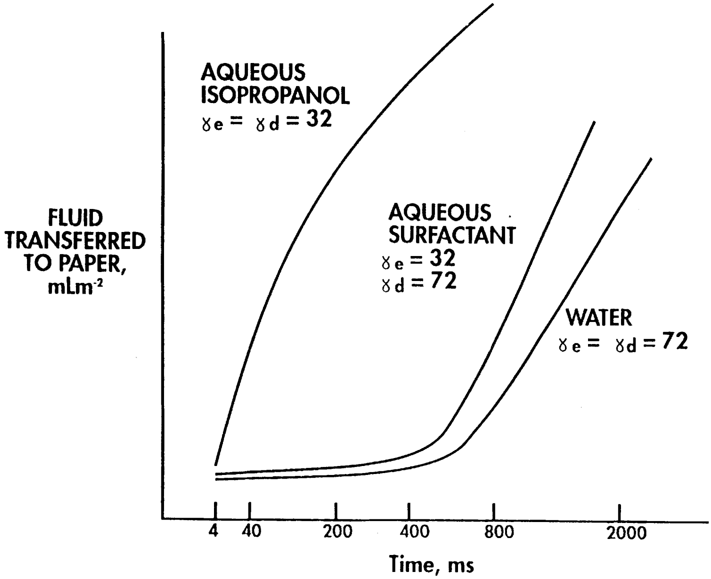

FIG. 7 Absorption curves for water, isopropyl alcohol in water, and a surfactant solution having the same equilibrium surface tension. The dynamic surface tension at a surface age of 3 mS is also shown. Aspler, Davis, and Lyne (36).

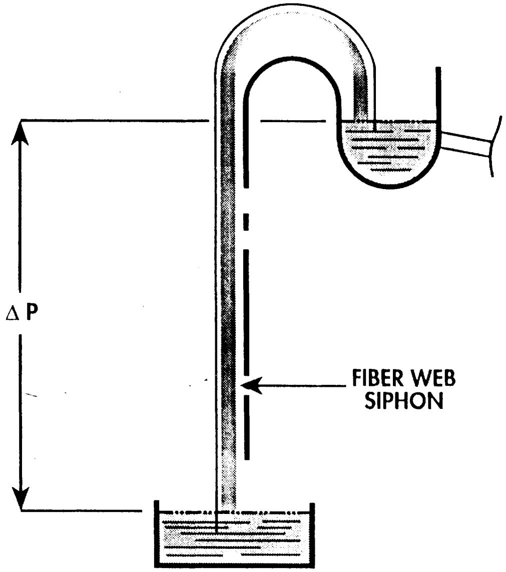

FIG. 8 Fiber web siphon for calculating permeability at saturation. Nguyen and Durso (21).

in water (thereby lowering surface tension) and spraying the liquid in drops onto paper using an ink jet printer they were able to monitor progress from non-penetration, to patchy penetration, to complete penetration at a constant time interval after the drops hit the paper. Of the fifteen copy papers they examined all but three showed broad concentration ranges where penetration was patchy. This outlines the inhomogeneity of the surface chemistry of sized fine paper and its effect on the uniformity of penetration of aqueous liquids. Considerable benefit to print uniformity would accrue from a more uniform application of size and the avoidance of "hot spots". The need for research in this area is becoming increasingly important with the accelerating trend to water-based inks.

PRESSURE PENETRATION

Darcy's law is invariably the starting point for any discussion of forced penetration of porous media:

$$v = K\Delta P/\mu L \qquad (5)$$

where v is the volumetric flow rate into the medium per unit area, K is the permeability, μ is the viscosity of the fluid, and $\Delta P/L$ is the pressure drop per unit of penetration distance. The assumptions inherent in this model of pressure flow limit its applicability. While pressure penetration of low density pulp pads such as those used in diapers can be modelled using Darcy's law, more anisotropic materials such as printing papers cannot be characterized by a unidimensional permeability factor.

Lindsey (20) examined the anisotropic permeability of paper using the following vector form of Darcy's law:

$$\mathbf{v} = -K\nabla P/\mu \qquad (6)$$

where **v** is now a velocity vector, ∇P is the pressure gradient, and K is a second order tensor of the form:

$$K = \begin{bmatrix} K_x & 0 & 0 \\ 0 & K_y & 0 \\ 0 & 0 & K_z \end{bmatrix} \qquad (7)$$

where K_x, K_y, and K_z are the permeability components in the x,y, and z directions (CD, MD, and transverse directions, respectively). The direction of flow need not be in the same direction as the pressure gradient in an anisotropic medium. Therefore, in order to calculate K_x, K_y, and K_z it is necessary to measure velocity and pressure drop in the same direction, and then calculate an apparent permeability in that direction. By repeating the process in different directions it is then possible to calculate K_x, K_y, and K_z via direction cosines. Since this is not practical experimentally, several investigators have opted to constrain the flow.

Nguyen and Durso (21) studied the flow in one direction by suspending the paper vertically and measuring the steady state flow down the saturated paper strip as a form of siphon (see Figure 8). ΔP in the vertical direction is then simply the hydrostatic head, and the permeability at saturation, K_o, can be calculated from the flow rate of liquid that is required to maintain a constant level in the reservoir above the sample. They also studied capillary flow in the vertical direction by dipping one end of the sample in a liquid reservoir and then cutting the sample into horizontal strips at different times after immersion. By weighing these strips they were able to assess the rate at which the permeability coefficient changed with the degree of saturation in the sample. As shown in Figure 9 their results confirmed the cubic relationship proposed by Gillespie (22) in his classic studies of imbibition in filter papers. Thus, it should be remembered that in most processes involving pulsed impression of liquids into paper, such as in printing or coating, there is a gradient in saturation that will influence local permeability. The rate at which the pore system in paper saturates locally under pressure penetration depends principally on the distribution of pore size and shape.

Lindsey (20), and Miller et al. (23) constrained the flow to the plane of the fiber web by compressing the sample between parallel plates. While Lindsey measured the amount of liquid pushed into the compressed fiber web under pressure, Miller weighed the amount drawn into the sample by an applied vacuum. Both were able to study the effect of varying sample compression on porosity and permeability.

Classically, investigators have used the Kozeny-Carmen equation to relate permeability to porosity:

$$K = \epsilon^3 d_e^2 / 36(1 - \epsilon)^2 \kappa \tag{8}$$

The Kozeny constant κ is set according to the type of pore structure, and ϵ is the void fraction in the fiber web calculated as $1 - m/V\rho$, where m is the mass of the sheet, V is the compressed volume between the parallel plates and ρ is the density of solid cellulose. The model assumes a uni-

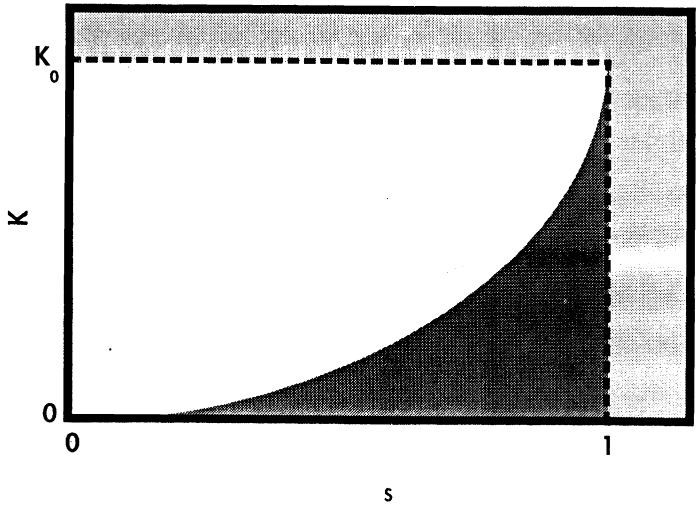

FIG. 9 Change in the permeability coefficient K with the degree of saturation s. Nguyen and Durso (21).

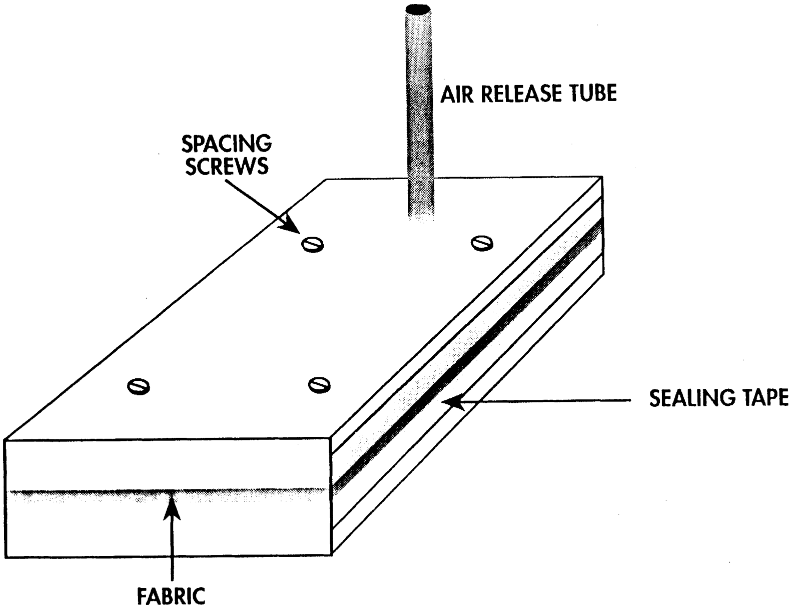

FIG. 10 Parallel plate permeability cell. Miller et al (23).

form bed of packed particles having an effective particle diameter of d_e. While the model works reasonably well for relatively simple structures such as woven polypropylene fabrics, it does not accommodate the complex, irregular and microscopically rough pore systems associated with machine made paper. Therefore, Lindsey (20) fit the permeability to the void fraction of paper samples using an exponential model, thereby avoiding the difficulty in setting the Kozeny constant and in establishing the actual physical volume of the sample. In either case, compression of the samples leads to a highly nonlinear reduction in permeability.

Lindsey (20) was able to show that the lateral permeability (K_x or K_y) of machine made papers exceeded the transverse permeability (K_z) by approximately a factor of two, and that the permeability in the machine direction was invariably greater than in the cross direction ($K_y > K_x$). Thus, liquids that are impressed into paper will have a natural tendency to spread in the plane of the web, forming an elliptical pattern orientated in the machine direction.

It should be remembered that these models also assume a uniform z-direction structure which is becoming less likely with modern forming, pressing, drying, surface sizing and pigmentization, and calendering methods. Structural variation in the x-y plane is also important in the avoidance of uneven pressure penetration, which can be a major cause of mottling and related phenomena. Thus, it would be useful to extend these permeability studies to models which more closely resemble real paper structure.

Many of the liquids impressed into paper during converting, printing, and end-use operations are non-Newtonian. Miller et al. (23) demonstrated that the penetration of an aqueous glycerol solution into a woven fabric followed a linear relationship between applied pressure and the square of the volume of liquid entering the sample per unit time over a broad range of applied pressures. However, an aqueous solution of polyacrylamide showed only a fraction of the penetration rate at higher pressures that would be expected by a linear extrapolation of its penetration behavior at low pressures. The onset of this non-Newtonian behavior could be determined as a function of the applied pressure in this manner.

As shown by Lyne and Aspler (24), a greater resistance to pressure penetration is desirable in printing because it leads to higher print density for the same amount of applied ink. Similarly, resistance to penetration during blade coating is desirable. Long chain polymers are commonly added to printing inks and coating colors in order to provide greater penetration resistance. However, it is not clear which rheological property, or properties predominate in this effect. Shear thickening, elasticity, and resistance to extensional flow may all play a role. Lyne (25) has pointed out that the surface pores in paper can be modelled as truncated cones, and thus, impression of liquids into the surface of paper involves extensional deformation. To the extent that polymeric additives can increase extensional viscosity on a time scale that is relevant to printing and coating it may be possible to significantly improve hold-out on porous stocks.

Lastly, paper and paperboard are often made sufficiently hydrophobic by hard sizing that liquids will not penetrate under a low hydrostatic pressure. For example, the exposed edges of a seamed milk carton must resist penetration of the milk or the stiffness of the board will decrease and the container will bulge. Miller et al. (23) have used the parallel plate compression cell pictured in Figure 10 to determine the critical pressure at which edge wicking of water begins.

Similarly, mercury has a sufficiently high surface tension (480 mN/m) that it must be pushed under considerable pressure to penetrate into the average pore size in paper. By recording the incremental increase in the amount of mercury that intrudes into paper as the driving pressure is increased it is possible to determine the distribution of the sizes of pore throats in the paper structure using the Washburn equation:

$$d = 4\gamma\cos\theta/P. \tag{9}$$

Since it is difficult to determine the contact angle θ for mercury with the irregular pore walls in paper, because of the high compressive pressures applied during the intrusion process, and since mercury must frequently penetrate into large cavities after being pushed through narrow throats, the interpretation of mercury intrusion data is not simple. Miller et al. (26) have introduced an elegant method of determining pore size distribution that does not compress the paper sample. As shown in Figure 11, the paper sample is suspended on a sintered membrane and is fully saturated with

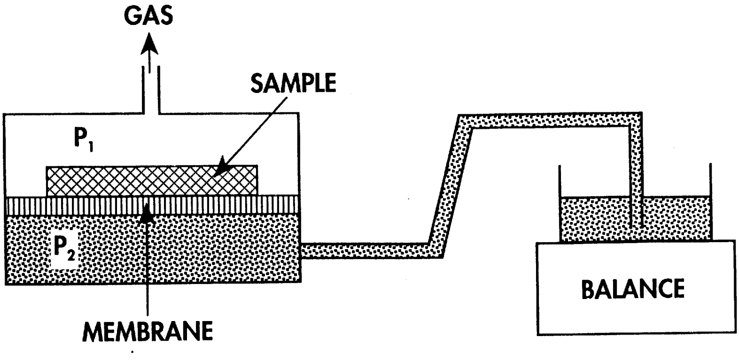

FIG. 11 Porosimeter in which a saturated paper sample is supported on a porous membrane and applied air pressure causes extrusion of liquid measured by balance at right. Miller et al (26).

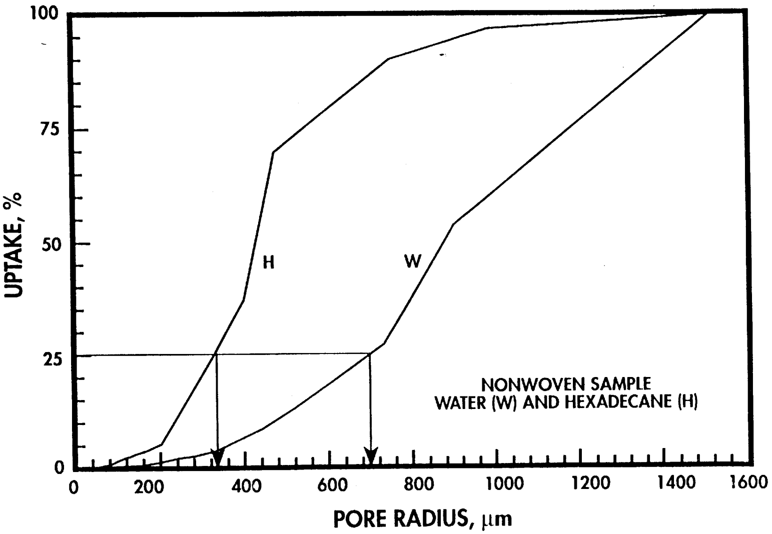

FIG. 12 Distribution of pore throats in nonwoven sample showing the effect of swelling of fibers on pore sizes. Miller et al (26).

the test liquid before the test begins. Air pressure is then applied in increments to the sealed chamber driving liquid from progressively smaller pores in the paper. By measuring the amount of liquid displaced with each pressure step it is possible to build up a pore size distribution diagram using the Washburn equation. Further, it is also possible to release the pressure incrementally and let the liquid back into the sample in a stepwise fashion. Advancing contact angles can be measured during the intrusion of a liquid, and receding contact angles measured during extrusion. Hysteresis for the intrusion and extrusion of the liquid can be used to deduce the distribution of bottleneck and transverse pores that are frequent in paper. Also, by making evaluations with water, and then with a non-swelling liquid such as hexadecane, the effect of swelling on the pore size distribution can be determined (see Figure 12).

This appears to be a valuable approach for analyzing the pore structure of paper down to a pore radius of about one micron. At the lower end of the sensitivity range air diffusion through the support membrane becomes problematic, but research is under way to extend the useful range of the instrument.

DIFFUSION INTO THE FIBER WALL AND SWELLING

Hardwood and softwood fibers consist primarily of cellulose, lignin, and various hemicelluloses. The bulk of a softwood tracheid is a helical winding of cellulose fibrils enrobed in hemicellulose called the secondary wall. The fibrillar angle and thickness of the secondary wall predominate in determining the rheological properties of the fiber. Chemical pulping and bleaching act to remove most of the lignin, and together with beating, make the fiber wall more accessible to water penetration.

The ultrastructure of the fiber wall consists of amorphous and ordered regions. Water can readily penetrate the amorphous regions where cellulose and hemicellulose behave like a gel and swell in proportion to the amount of water absorbed.

Diffusion of water into the fiber wall, or into paper that has been densified to the point of becoming a translucent solid is driven by a concentration gradient (dC/dx) and can be modelled by Fick's Second Law:

$$dC/dt = Dd^2C/dx^2 \qquad (10)$$

where D is the diffusion coefficient, and t denotes time.

Hydrogen bonding between the cellose chains controls the ordering in the semi-crystalline regions of the fibrillar structure. Water can break hydrogen bonds in these regions but hydration occurs so slowly that it is not significant on the time scale of printing and coating. Swelling results in an expansion of the fiber, and because of the helical structure of the secondary wall expansion occurs principally in the radial direction. Thus, the fiber length changes typically about one thirtieth that of the fiber cross section.

In a normal machine-made paper a high percentage of the fiber surface is attached to other fibers via interfiber hydrogen bonds. Since the fibers shrink radially during drying in the papermaking process it also follows that shrinkage stresses must develop at fiber crossings and, thereby, the entire fiber network shrinks during drying.

Softwood tracheids have aspect ratios in the order of 100 and thus have a strong tendency to align in the direction of flow during the forming process in papermaking. Fiber orientation in the direction of manufacture and the tension used to draw the paper web through the papermachine cause machine made papers to exhibit greater shrinkage and hygroexpansion in the cross-direction than in the machine direction.

As a general rule, anything which acts to increase the bonded area between fibers will increase network hygroexpansion, and vice versa. For example, increased beating or wet pressing, and the addition of fines or cationic starch will increase hygroexpansion while the addition of filler will disrupt interfiber bonding and decrease hygroexpansion. In general, however, hygroexpansion cannot be reduced significantly by varying these factors since other paper properties such as strength will be adversely affected.

Hygroexpansion is particularly undesirable during printing as it leads to misregistration of colored halftones (especially across the width of a printing press), sheet handling problems caused by curl and cockle, and difficulty in maintaining tolerances for hole punching etc. in forms printing. The cause of hygroexpansion in offset lithography is the absorption of aqueous

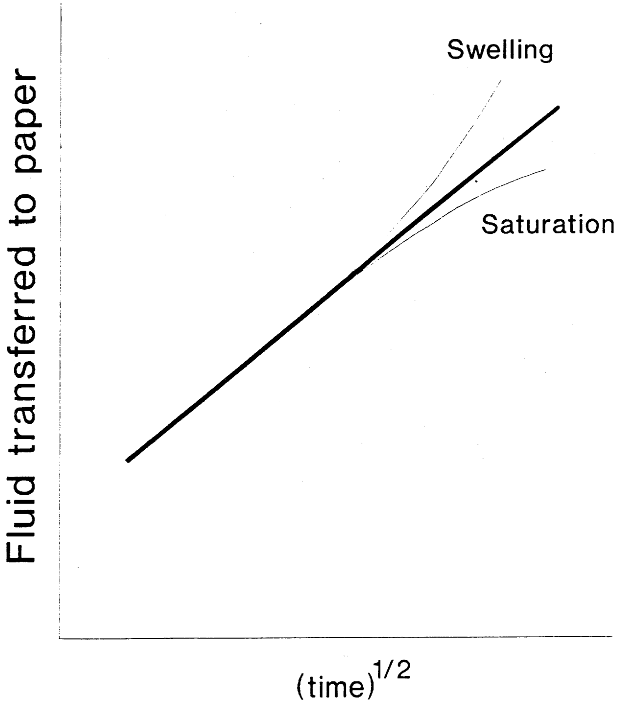

FIG. 13 Effect of fiber swelling on the rate of penetration of water into paper in a Bristow absorption test.

fountain solution borne by the ink and through transfer in non-image areas. With a growing trend to water-based printing comes increased pressure to minimize hygroexpansion. This translates into a quest to reduce fiber swelling, at least during the time scale of printing operations.

As shown in Figure 13, the onset of water penetration into the fiber wall and associated network swelling can be seen as a deviation upwards in the rate of penetration (slope) in a Bristow absorption curve. If water penetrates only into interfiber pores, then no swelling or network expansion takes place on the time scale of the test (nominally, 2 seconds). However, if absorption into the fiber wall occurs on this time scale the resulting network expansion will cause an increase in the size of interfiber pores and an associated increase in the rate of penetration.

Penetration of water into the fiber wall can be delayed by the addition or application of hydrophobic sizing agents. However, water-based inks, varnishes, coatings, and offset fountain solution must be sorbed to some degree in order to facilitate transfer, setting and/or drying. Thus, it is generally not advisable to size so hard that water cannot penetrate interfiber pores in the fiber network. A more practical solution to the hygroexpansion problem is to limit swelling of the fibers by suitable chemical treatment.

Esterification of carboxyl groups in wood pulps (Scallan [27]) and acetylation of wood pulps (Klinga and Tarkow [28]) can reduce swelling and hygroexpansion by as much as 50 percent. Presumably, creating ether linkages between hydroxyl sites on the cellulose chain would also reduce swelling and hygroexpansion. However, fiber swelling aids in establishing the conformation and close contact between fibers that is necessary for the establishment of interfiber hydrogen bonding. Thus, these treatments would have to be performed after the paper was dried in order to avoid loss of bonding and sheet strength.

Hardboard made from mechanical pulps is normally heat treated for up to several hours in order to increase wet strength and reduce hygroexpansion. Bristow and Back (29) speculated that heat treatment induced autocrosslinking in the hardboard. Zhou et al. (30) have described a more practical way to crosslink cellulose in chemical wood pulps. Treatment with butane-tetracarboxylic acid and a phosphate catalyst reduced hygroexpansion by 40 percent in TAPPI handsheets made with a 50/50 blend of bleached softwood/hardwood kraft pulp (a typical fine paper furnish).

The swelling of fibers in a dry sheet of paper and the associated hygroexpansion may be reduced by pre-drying the pulp, or by removal or degradation of hemicellulose in pulp as in the manufacture of alpha cellulose. It has also been know since the work of Cohen et al. (31) in 1949 that swelling can be reduced by increasing ionic concentration in the pulp. More recent work by Scallan and Grignon (32) and Lindstrom and Carlsson (33) showed that by exchange of the calcium ions normally present in wood pulps for higher valence ions such as Al^{3+} swelling could be significantly reduced. However, in all of these cases the fibers become stiffer and less conformable during papermaking with an attendant loss of sheet strength. Were any of these approaches to reduction of hygroexpansion to be commercially successful, the loss of interfiber bonding would have to be compensated by the addition of a bonding agent to the furnish such as cationic starch or fines.

Research into minimizing hygroexpansion without compromising other key performance characteristics or adding significant cost should be given high priority since hygroreactivity is a critical disadvantage to the use of paper and board as a printing medium in the coming water-based era.

CONCLUSIONS

Papermakers have relied on models for wetting, capillary adsorption, and pressure penetration that do not apply to structures as complex as those found in uncoated and coated paper and board. Further, wetting and adsorption models such as Young's spreading equation and the Lucas-Washburn equation are thermodynamically based and totally inappropriate for most industrial or commercial processes which are highly dynamic and usually involve the application of external forces to the system.

Some recent advances in understanding of the dynamic interactions of liquids with solid surfaces have been reviewed. Much work lies ahead before the interactions of liquids which are impure mixtures with surfaces which are heterogeneous and morphologically complex can be modelled under conditions that prevail in paper's many end-uses. However, modern acid-base theory, morphologically specific capillary models, rheological models for polymer solutions, three dimensional pressure penetration models, and an understanding of the factors controlling the swelling of cellulose can be of immediate assistance in designing paper and board products for an ever more demanding marketplace.

AKNOWLEDGEMENTS

The author gratefully acknowledges the assistance of Dr. Yan Huang in the preparation of this manuscript, and would like to thank Professor Börje Steenberg for reviewing its contents.

REFERENCES

1. Aspler, J. S., DeGrace, J.H., Beland, M.C., Maine, C., and Piquard, L., "Transfer and Setting of Water-Based Ink, Part II", J. Pulp and Paper Sci., in press.

2. van Oss, C.V., J. Dispersion Sci. and Tech., 12(2): 201-219 (1991).

3. Lyne, M.B. and Huang Y.C., "Measuring Acid-Base and Dispersive Interactions with Paper Surfaces under Dynamic Conditions", Nordic Pulp and Paper, in press.

4. Huang, Y.C., and Lyne, M.B., "The Dependence of Dispersive Interactions on Capillary Pressure", to be submitted.

5. Hardy, W.B., Phil. Mag. 38: 49 (1919).

6. Marmur, A. and Lelah, M.D., Chem. Eng. Commun., 13: 133-143 (1981).

7. Leger, L., Erman, M., Guinet-Picart, A.M., Ausserre, D., Strazielle, C., Benattar,J.J., Rieutord, F., Daillant, J., and Bosio, L., Revue Phys. Appl. 23: 1047-1054 (1988).

8. deGennes, P.G., Rev. Mod. Phys. 57(3):827-862 (1985)

9. Lelah, M.D. and Marmur, A., J. Coll. & Int. Sci. 82(2): 518-525 (1981).

10. Lyne, M.B. and Aspler, J.S., Tappi 65(12): 98-101 (1982).

11. Borgin, K., Norsk Skogindustri 13(11):429-442 (1959).

12. Oliver, J.F. and Mason, S.G., J. Coll. & Int. Sci. 60: 480 (1977).

13. Cazabat, A.M. and Cohen Stuart, M.A., Progr. Coll. & Polymer Sci. 74: 69-75 (1987).

14. Kent, H.J. and Lyne, M.B., Nordic Pulp and Paper Res. J., 4(2): 141-145 (1989).

15. Corte, H. and Kallmes, O.J., in The Formation and Structure of Paper, (F. Bolam ed.) Tech. Div., B.P.B.I.F., London, p. 351, (1962).

16. Okayama, T., Kimura, S. and Oye, R., Japan Tappi, 60(12): 57-63 (1985).

17. Marmur, A., Adv. in Coll. & Int. Sci. 39:13-33 (1992).

18. Gibbs, J.W., The Scientific Papers, Vol. 1, p288, New York, Dover (1961).

19. Borhan, A., Pence, S.B. and Sporer, A. H., J. Imaging Tech. 16(2): 65-69 (1990).

20. Lindsay, J.D., "The Anisotropic Permeability of Paper: Theory, Measurements, and Analytical Tools", IPC Tech. Paper Series # 298 (1988).

21. Nguyen, H.V. and Durso, D.F., Tappi, 66(12): 76-79.

22. Gillespie, T., J. Coll. Sci., 14:123 (1959).

23. Miller, B., Friedman, H. L. and Amundson, R., proceedings of Tappi Nonwovens Conference, p. 19 (1991).

24. Lyne, M.B. and Aspler, J.S., ACS Symp. Series # 200 on Colloids and Surfaces in Reprographic Technologies, Chap. 20, pp.385-420 (1981).

25. Lyne, M.B., in Advances in Printing Science and Technology, W.H. Banks ed., Pentech, Vol. 20, pp.36-248 (1990).

26. Miller, B., Tyomkin, I, Wesson, S.P., and Mahale, A.D., Interactions of Fluids with Fibrous Materials, Textile Research Institute Report #49, Princeton, (1992).

27. Scallan, A.M., Tappi, 66(11):73-75 (1983).

28. Klinga, L.O. and Tarkow, H., Tappi, 49(1):23-27 (1966).

29. Bristow, A.J. and Back, E. L., Sv. Papperstidning, 72(11):367-374 (1969).

30. Zhou, Y.J., Luner, P. and Caluwe, P., "Wet Reinforcing of Paper and Board with Novel Crosslinking Chemicals", in proceedings of 1990 Fundamental Research Symposium, Oxford.

31. Cohen, W.E., Farrant, G. and Watson, A.J., Appita Proc. 3:72 (1949).

32. Scallan, A.M. and Grignon, J., Sv. Papperstidning, 82(2):40-47 (1979).

33. Lindström, T. and Carlsson, G., Sv. Papperstidning, 85(3): R14-20 (1982).

34. DeGrace, J.H. and Mangin, P.J., in Advances in Printing Sci.& Tech., W.H. Banks ed., Pentech, Vol. 17, pp. 312-332 (1983).

35. Kent, H.J. and Lyne, M.B., in Fundamentals of Papermaking, Mech. Eng. Publ. Ltd., C.F. Baker ed., pp. 895-920 (1989).

36. Aspler, J.S., Davis, S. and Lyne, M.B., J. Pulp & Paper Sci., 13(2): J55-60 (1987).

Transcription of Discussion

ON THE INTERACTIONS OF LIQUIDS WITH PAPER UNDER DYNAMIC CONDITIONS

ADDENDUM TO TABLE 1

Note the extra line below in Table 1 for cellophane conditioned to 15% RH.

Hydrophilicity and Acid-Base Interactions

Substrate	γ_S^{LW} (mN/m)	Contact Angle with Water (deg.)	W_A (mJ/m²)	W_A^d (mJ/m²)	W_A^{ab} (mJ/m²)
Glass	76.0	0	145.6	81.4	64.2
Cellophane (15% RH)	50.2	68	100.1	66.2	33.9
(50% RH)	48.6	28	137.1	65.1	72.0
(95% RH)	41.6	5	145.3	60.2	85.1

ADDENDUM TO FIGURE 6

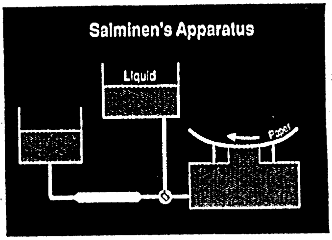

Figure 6(a) Salminen's apparatus for atmospheric and pressure penetration of liquids into paper. Figures 6(a) and 6(b) from: P.J. Salminen, "Water transport into paper - the effect of some liquid and paper variables." Tappi 71(9):195-200 (1988).

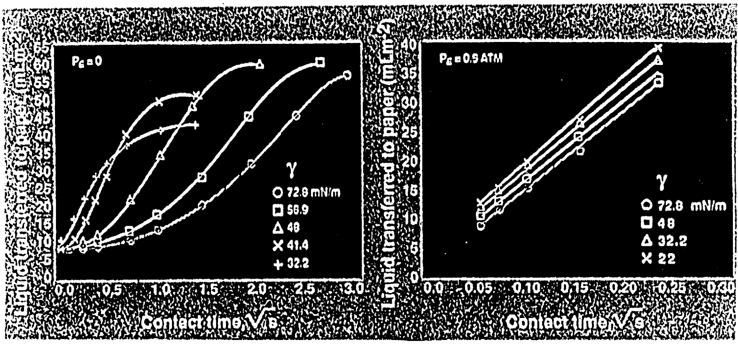

Figure 6(b) Comparison of atmospheric sorption (P_E=0) and penetration under 0.5 atmospheres external pressure of water and aqueous isopropanol solutions into LWC base paper. Note that the effect of surface tension on sorption virtually disappears when an external pressure is applied. This begs the question as to what pressure is just sufficient to overcome surface energetics and cause wetting.

ADDENDUM TO FIGURE 7

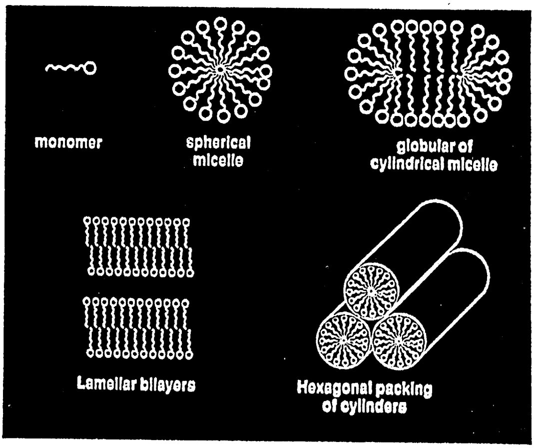

7(a) It is possible to choose surfactants that migrate more rapidly to a newly created liquid surface and affect sorption rates on a shorter time scale than that shown in Figure 7. The rate of migration and dynamic surface tension at short time intervals depends principally on the size of the surfactant molecule. However, above a critical concentration the surfactant molecules tend to aggregate in micellar structures with polar heads facing outwards. Since the micelles are much larger than the surfactant monomer this aggregation can significantly slow migration, and the monomer concentration will not increase with addition of more monomer after the critical micelle concentration is reached. Thus, even a relatively small surfactant molecule may exhibit a high dynamic surface tension if the critical micelle concentration is too low. Shown above are some idealized micelle configurations which the surfactant monomer may tend towards as the concentration is increased above the critical threshold.

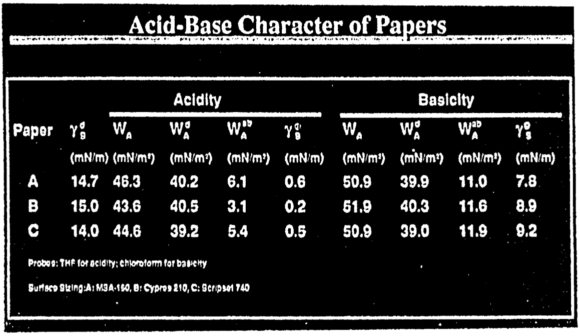

Acid-Base Character of Papers

		Acidity				Basicity			
Paper	γ_S^d (mN/m)	W_A (mN/m²)	W_A^d (mN/m²)	W_A^{ab} (mN/m²)	$\gamma_S^{a'}$ (mN/m)	W_A (mN/m²)	W_A^d (mN/m²)	W_A^{ab} (mN/m²)	γ_S^{e} (mN/m)
A	14.7	46.3	40.2	6.1	0.6	50.9	39.9	11.0	7.8
B	15.0	43.6	40.5	3.1	0.2	51.9	40.3	11.6	8.9
C	14.0	44.6	39.2	5.4	0.5	50.9	39.0	11.9	9.2

Probes: THF for acidity; chloroform for basicity

Surface Sizing: A: MSA-150, B: Cypres 210, C: Scripset 740

Table showing the dispersive and acid-base character of the surface of an alkaline fine paper treated with three different surface sizes. Note that the acid character of the surface changes most from one size to another. From ref. # 3, M.B. Lyne and Y.C. Huang, Nordic Pulp & Paper, 8(1): 120-22 (1993)

I Kartovaara, Enso-Gutzeit Oy, Finland

I would like to make a comment and ask a question. The comment is about the applicability of the Lucas-Washburn equation. It is a steady state equation where you equate the driving force, the surface tension and the viscous drag. In the very beginning of the penetration the viscous drag becomes zero. Then you get the absurd result that the penetration rate is infinite. This has been treated in the literature and it shows that when the penetration is only a few pore diameters you must make corrections and I think in our applications the penetration depth can be only a few pore diameters. So the Lucas-Washburn equation is not applicable in those instances.

B Lyne

I came not to praise the Lucas-Washburn equation but to bury it, and I agree that the boundary conditions are absurd in this equation. Even more important, is the fiction that a single parameter R can represent the incredibly complicated structure in paper. We must look beyond such a simple model because the pore form has a great deal of influence on the penetration.

I Kartovaara

The question is about the measurement of contact angle - like you have shown – it is very dependent on the atmosphere -how much water vapour that has already wetted the surface.

What is your recommendation is it sufficient to measure it in different relative humidities - should we also change temperature - how should be measure the contact angle?

B Lyne
If you use two fluids, one which has a virtually zero advancing contact angle, and then the fluid you are interested in (it must be a non-swelling liquid so you have the same structure in both cases) then you can measure the dynamic advancing contact angle during liquid penetration in the Bristow test, whereas it is very difficult to measure a static contact angle on the surface of paper with low surface tension liquids. Yaw Huang and I did that in the paper dealing with the calculation of acid base character of paper (Ref. 3).

Prof P Stenius, Helsinki University of Technology, Finland
I am interested in your interpretation of the effect of relative humidity on cellulose chemistry in terms of acid-base interactions. Cellulose swells considerably with water at 50-95% humidity. From the measured values for the dispersive and acid-base contributions you infer that as you go from 50 to 95% relative humidity the work of adhesion as well as its dispersion and acid-base (or polar) parts approaches the values of water itself. Are you not in fact just detecting that the surface becomes more and more covered with water so that you are eventually measuring the cohesive energy of water?

B Lyne
There is an extra line for Table 1 which appears in the Addendum for 15% relative humidity. When you look at the absorption isotherm for water on cellulose, down at 15% RH you are seeing strongly bound water and when you go to 95% you are seeing multi-layers or free water on the surface. In moisturising cellulose you are certainly moving from a situation where water has a strong influence on the surface chemistry of cellulose to just dealing with free water at the

upper end. That is why at 95% RH the work of adhesion is exactly equal to the work of cohesion for water. So, I agree with your comment.

Dr L Wagberg, SCA Research AB, Sweden
I have a couple of minor comments first and then a question. When talking about the equipment of Tyomkin and Miller you mention in the text they used the Washburn equation but actually they are using the La Place equation to calculate the distribution.

B Lyne
I stand corrected.

L Wagberg
The second comment refers to the curves you show in figure 12. Your discussion is correct ie that the equipment can be used to study sheet expansion upon exposure to water and that shows you cannot use Bristow equipment to detect contact angles with water.

B Lyne
I hope I said earlier that you have to use a fluid that is non interactive with cellulose (ie non-swelling) when measuring contact angles in the Bristow test because the structure must remain the same for the two fluids. If you have an interactive fluid the structure will change.

L Wagberg
But what figure 12 actually is showing, with these two curves, is the difference in contact angle between hexadecane and water. It is actually the major point and not swelling which is very low for the

sample shown. The question is - Page 893 Fig.4. You write in the text that there is an acceleration of a liquid into a converging pore. Is this really so? Your discussion is mainly about the change in the driving pressure changed contact angle and that in turn is dependent on the geometry. But as the liquid starts to flow there is an opposing force as well, caused by the viscous drag.

B Lyne

The viscous drag is larger in a smaller pore, and the penetration rate is proportional to the pore radius, even though the capillary pressure is higher in the smaller pore. However, where the penetrating liquid has a contact angle near 90° and the liquid enters a conical pore, or convergent portion of a pore, there is an observable jump or acceleration in penetration rate. This is because the sudden increase in curvature of the liquid reflects a jump in capillary pressure without an immediate reduction in pore radius or increase in drag. This increase in capillary pressure will outweigh increase in drag for the short conical sections of pores found in paper.